Revitalization of a Forward Genetic Screen Identifies Three New Regulators of Fungal Secondary Metabolism in the Genus *Aspergillus*

Brandon T. Pfannenstiel,[a] Xixi Zhao,[b,c] Jennifer Wortman,[d*] Philipp Wiemann,[b]
Kurt Throckmorton,[a*] Joseph E. Spraker,[e*] Alexandra A. Soukup,[a*] Xingyu Luo,[e]
Daniel L. Lindner,[f] Fang Yun Lim,[b] Benjamin P. Knox,[b] Brian Haas,[d]
Gregory J. Fischer,[a*] Tsokyi Choera,[b] Robert A. E. Butchko,[g] Jin-Woo Bok,[b]
Katharyn J. Affeldt,[b*] Nancy P. Keller,[b,h] Jonathan M. Palmer[f]

Department of Genetics, University of Wisconsin—Madison, Madison, Wisconsin, USA[a]; Department of Medical Microbiology and Immunology, University of Wisconsin—Madison, Madison, Wisconsin, USA[b]; School of Life Sciences, Sun Yat-Sen University, Guangzhou, China[c]; Genome Sequencing and Analysis Program, Broad Institute of MIT and Harvard, Cambridge, Massachusetts, USA[d]; Department of Plant Pathology, University of Wisconsin—Madison, Madison, Wisconsin, USA[e]; Center for Forest Mycology Research, Northern Research Station, U.S. Forest Service, Madison, Wisconsin, USA[f]; Department of Plant Pathology and Microbiology, Texas A&M University, College Station, Texas, USA[g]; Department of Bacteriology, University of Wisconsin—Madison, Madison, Wisconsin, USA[h]

ABSTRACT The study of aflatoxin in *Aspergillus* spp. has garnered the attention of many researchers due to aflatoxin's carcinogenic properties and frequency as a food and feed contaminant. Significant progress has been made by utilizing the model organism *Aspergillus nidulans* to characterize the regulation of sterigmatocystin (ST), the penultimate precursor of aflatoxin. A previous forward genetic screen identified 23 *A. nidulans* mutants involved in regulating ST production. Six mutants were characterized from this screen using classical mapping (five mutations in *mcsA*) and complementation with a cosmid library (one mutation in *laeA*). The remaining mutants were backcrossed and sequenced using Illumina and Ion Torrent sequencing platforms. All but one mutant contained one or more sequence variants in predicted open reading frames. Deletion of these genes resulted in identification of mutant alleles responsible for the loss of ST production in 12 of the 17 remaining mutants. Eight of these mutations were in genes already known to affect ST synthesis (*laeA*, *mcsA*, *fluG*, and *stcA*), while the remaining four mutations (in *laeB*, *sntB*, and *hamI*) were in previously uncharacterized genes not known to be involved in ST production. Deletion of *laeB*, *sntB*, and *hamI* in *A. flavus* results in loss of aflatoxin production, confirming that these regulators are conserved in the aflatoxigenic aspergilli. This report highlights the multifaceted regulatory mechanisms governing secondary metabolism in *Aspergillus*. Additionally, these data contribute to the increasing number of studies showing that forward genetic screens of fungi coupled with whole-genome resequencing is a robust and cost-effective technique.

IMPORTANCE In a postgenomic world, reverse genetic approaches have displaced their forward genetic counterparts. The techniques used in forward genetics to identify loci of interest were typically very cumbersome and time-consuming, relying on Mendelian traits in model organisms. The current work was pursued not only to identify alleles involved in regulation of secondary metabolism but also to demonstrate a return to forward genetics to track phenotypes and to discover genetic pathways that could not be predicted through a reverse genetics approach. While identification of mutant alleles from whole-genome sequencing has been done before, here we illustrate the possibility of coupling this strategy with a genetic screen

to identify multiple alleles of interest. Sequencing of classically derived mutants revealed several uncharacterized genes, which represent novel pathways to regulate and control the biosynthesis of sterigmatocystin and of aflatoxin, a societally and medically important mycotoxin.

KEYWORDS *Aspergillus nidulans*, forward genetics, whole-genome sequencing, secondary metabolism

Due to its carcinogenic, mutagenic, and teratogenic properties, the fungal secondary metabolite aflatoxin has warranted the attention of many research groups with the goal of understanding its regulation and biosynthesis (1–3). Several species of *Aspergillus* can produce aflatoxin, which was originally discovered as the cause of the 1960 Turkey X disease (4). Chronic exposure to aflatoxin is known to lead to liver disease and cancer and is associated with immunological deficiencies in certain populations of the developing world (2, 5, 6). Understanding the genetic regulation of aflatoxin production, with the goal of developing strategies to reduce contamination of food and feed, has been an area of intense interest.

A hallmark of fungal secondary metabolites is that genes involved in production of a particular metabolite are clustered at a genetic locus, typically called a secondary metabolite cluster or biosynthetic gene cluster (BGC) (7). *Aspergillus flavus* and *A. parasiticus* contain nearly identical BGCs that are responsible for aflatoxin biosynthesis, while the genetic model *A. nidulans* harbors a similar BGC that produces the penultimate aflatoxin precursor sterigmatocystin (ST) (8). A critical finding for ST and aflatoxin regulation was the characterization of one of the cluster genes, *aflR*, which encodes a cluster-specific transcription factor that positively controls expression of biosynthetic genes within each respective cluster (9–11). The interchangeability of *aflR* homologs between *A. nidulans* and *A. flavus* was one of the first demonstrations that analyzing ST regulation in *A. nidulans* could be used as a model for aflatoxin regulation (11). Since then, *A. nidulans* has emerged as an important system for studying genetic regulation of secondary metabolism in general (12, 13).

To identify regulators of the ST BGC in *A. nidulans*, a forward genetic screen was designed to identify mutants deficient in ST production resulting from mutations located outside the gene cluster (14). This was achieved by chemical mutagenesis of an *A. nidulans* Δ*stcE* strain which accumulates the first stable ST/aflatoxin intermediate, norsolorinic acid (NOR). NOR acts as a proxy for measuring ST and is advantageous as a screening molecule because it is visible to the unaided eye as an orange pigment (see Fig. S1 in the supplemental material). The study resulted in the identification of 23 MRB (mutagenesis Robert Butchko) mutants that were reduced in their ability to produce NOR with mutations that were not linked to the ST cluster. Subsequent classical genetic approaches (chromosomal mapping and cosmid library complementation) identified two genes from this original work, *mcsA* and *laeA*, respectively (15, 16).

Five of the 23 MRB strains mapped to the *mcsA* gene (17), which encodes a methylcitrate synthase required for converting propionyl-coenzyme A (propionyl-CoA) and oxaloacetate to 2-methylcitrate. ST and aflatoxin are examples of polyketides, a class of secondary metabolites, which are typically synthesized by successive condensations of malonyl-CoA units to a starter acetyl-CoA unit. However, other acyl-CoAs (e.g., propionyl-CoA) can initiate and interfere with polyketide synthesis (17). Mutations in *mcsA* lead to accumulation of propionyl-CoA, the substrate of methylcitrate synthase, which subsequently acts to block synthesis of ST and other polyketides produced by *A. nidulans* (15). Further studies demonstrated that feeding primary metabolites, or growing the fungus under conditions that increased intracellular pools of propionyl-CoA, decreased polyketide synthesis in the fungus (15). This work was instrumental in establishing the importance of primary metabolite pools in secondary metabolite synthesis (15, 17).

The second characterized mutant that arose from this screen was termed *laeA*, for loss of *aflR* expression (16). Deletion of *laeA* resulted in loss of ST production in

A. nidulans as well as loss of aflatoxin in *A. flavus* (16, 18). LaeA has since been shown to be a master regulator of secondary metabolism in many filamentous fungal species as well as a virulence factor in both animal- and plant-pathogenic fungi (18–22). A major advance in understanding LaeA function arose from the finding that it is a member of a conserved fungal transcriptional heterotrimeric protein complex, termed the "velvet complex" after its founding member VeA (velvet protein A) (23–25). The velvet complex mediates fungal developmental responses to environmental signals and is conserved in all filamentous Ascomycetes spp. examined to date (24, 26).

Further attempts to identify the causative mutation in the remaining 17 MRB mutants through classical complementation with a cosmid library failed. These uncharacterized MRB mutants were cryogenically stored, awaiting a faster and more economical strategy for identification. Whole-genome sequencing has been used to identify mutant alleles in multiple model organisms (27–29), including several fungi (30–35). Here we describe our success in utilizing next-generation sequencing of mutants using Illumina and Ion Torrent platforms to quickly and effectively identify the genetic basis of 12 of the remaining MRB mutants. We further show that the three new alleles identified from this screen show a conserved regulatory function in aflatoxin synthesis in *A. flavus*.

RESULTS

Next-generation sequencing and single nucleotide polymorphism (SNP) detection. Mutagenesis screens utilizing 4-nitroquinoline 1-oxide (4-NQO) typically produce single nucleotide mutations, with a preference for guanine-to-adenine (G-A) transitions. Estimations of the number of mutations induced by treatment with 4-NQO are dependent on the length of exposure and the subsequent kill rate; however, it has been predicted that current practices using 4-NQO are sufficient to reach saturation of screens (36). One major challenge in using whole-genome sequencing data to find a mutation causing the phenotype of interest is the presence of variants that do not influence that phenotype (background). Additionally, *A. nidulans* has been used as a genetic model for more than 50 years and, as a result, laboratory strains have been mutagenized many times to generate auxotrophic genetic markers, so it is expected that a "wild-type" strain from each *Aspergillus* research laboratory might harbor many background mutations in comparison to the genome reference FGSCA4 strain. Therefore, we utilized a series of backcrosses (two to seven) and resequenced a nearly isogenic "wild type" to remove background mutations.

Whole-genome sequencing using the Ion Torrent platform yielded 7× to 28× coverage per isolate, and we generated 39× coverage of MRB234 using Illumina GAIIx. We then created an SNP detection workflow using CLC Genomics Workbench that allowed rapid processing of the sequence data. Because we backcrossed the MRB mutants to the same parental strain, we created a database consisting of 4,329 variants that were found in more than one isolate and therefore likely constituted background mutations. Using this variant database and detection workflow, we filtered potential causative variants for each resequenced strain. This combined workflow resulted in identification of putative variants in 16 of 17 mutants sequenced; those strains where we could identify variants had a range of 1 to 21 per isolate. The use of backcrossing to create an isogenic background with our SNP detection workflow drastically reduced the number of potential mutants that needed to be manually curated and subsequently experimentally validated (Table 1; see also Table S1 in the supplemental material).

Identification of genes required for NOR production. With the assumption that a variant in a predicted gene would lead to a loss of function, we took advantage of rapid gene deletion using the ΔnkuA background in *A. nidulans* (37) and deleted all genes harboring nonsynonymous mutations for each MRB mutant. Genes were deleted in a NOR-accumulating strain, RAAS233.2, by replacing the predicted open reading frame with a copy of *pyrG* from *Aspergillus fumigatus* (see Fig. S1 in the supplemental material). The resulting transformants were assessed on NOR production medium

TABLE 1 Summary of 23 mutants identified in original genetic screen[a]

Strain	Gene ID(s) (product)	NGS	No. of BC	No. of AR	No. of ABP	Cov.	No. of Var.	No. Fil.	No. AAC Fil.	No. SNV Fil.	No. Man. Val.
MRB230	**AN9517 (SntB)**	Ion PGM	2	1,749,801	398,603,893	13×	2,753	454	200	8	6
MRB234	**AN4699 (LaeB)**	Illumina	5	12,853,110	1,178,389,385	39×	1,796	304	57	18	3
MRB246	**McsA** (classical)					0×					
MRB263	**AN4699 (LaeB)**	Ion PGM	4	716,799	183,494,864	6×	5,355	2,763	1,374	21	3
MRB265	**AN7825 (StcA)**	Ion PGM	2	1,670,811	393,800,438	13×	2,964	614	283	9	5
MRB278	**McsA** (classical)					0×					
MRB283	**AN0807 (LaeA)**	Ion PGM	7	1,637,954	414,891,029	14×	4,519	1,419	774	5	3
MRB285	**AN6650 (McsA)**	Ion PGM	7	2,040,309	504,104,294	17×	3,947	999	534	7	1
MRB288	**McsA** (classical)					0×					
MRB298	**AN0807 (LaeA)**	Ion PGM	7	1,432,539	398,442,512	13×	3,996	1,162	588	2	1
MRB300	**LaeA** (classical)					0×					
MRB303	**AN5169 (Ham9)**	Ion PGM	7	3,119,428	868,022,060	28×	2,470	178	88	1	1
MRB308	**McsA** (classical)					0×					
MRB311	**AN4819 (FluG)**	Ion PGM	7	2,688,125	757,320,587	25×	2,592	242	95	3	2
MRB320	**AN1932 (MsrB)**	Ion PGM	7	1,155,670	301,316,258	10×	2,908	870	397	1	1
MRB326	No mutation found (sequenced 2×)	Ion PGM	5	2,873,911	542,833,477	18×	2,606	120	29	4	0
MRB327	AN6374, AN6349, AN6309, AN6304	Ion PGM	5	825,533	212,012,177	7×	5,024	2,239	1,122	15	4
MRB333	**AN0807 (LaeA)**	Ion PGM	7	1,803,971	448,099,605	15×	4,927	1,711	996	7	0
MRB346	**AN0807 (LaeA)**	Ion PGM	6	1,602,269	410,313,827	13×	2,672	575	252	13	5
MRB357	**AN0807 (LaeA)**	Ion PGM	7	1,677,400	455,565,824	15×	3,301	575	298	4	3
MRB365	AN7084, AN7064, AN0850, AN0411, AN2194	Ion PGM	7	1,591,690	431,720,633	14×	3,302	605	307	11	5
MRB369	AN7034, AN6798, AN10042, AN3394	Ion PGM	2	1,680,284	391,401,260	13×	2,816	552	260	8	4
MRB379	**McsA** (classical)					0×					

[a]Boldfaced text in column two indicates which gene was found to be responsible for the loss of NOR production. Abbreviations are as follows: ID, identifier; NGS, next-generation sequencer; BC, backcrosses; AR, aligned reads; ABP, aligned base pairs; Cov., coverage; Var., variants; Fil., filtered; AAC, amino acid changes; SNV, single nucleotide variant; Man. Val., manually validated.

(oatmeal agar) and screened by eye for a loss of orange pigmentation. Deletions in six genes, three of which (*laeA*, *mcsA*, and *fluG*) were known to be required for ST biosynthesis, resulted in loss of NOR production (Fig. 1) (15, 16, 38). The other three genes, AN4699, AN5169, and AN9517, were uncharacterized (Fig. 1). The gene deletion and the subsequent loss of NOR production in these six strains explain the phenotype seen in 12 of the 17 MRB sequenced strains, as multiple strains harbored mutations in *laeA* and AN4699 (Table 1) (Table S1).

Complementation of sequenced strains confirms the presence of loci leading to loss of NOR production. To further confirm those loci identified by our deletion strategy as responsible for NOR production, we complemented the mutations in the backcrossed and sequenced MRB strains. To complement each strain, we cloned a full copy of each predicted gene with its native promoter and 3′ untranscribed region (UTR) into a plasmid with either a *metG* or *biA* selectable marker, depending upon the sequenced strain. These plasmids were then used to transform and complement the corresponding NOR mutant. Each sequenced strain was also transformed with a plasmid containing only a selectable marker to create a prototrophic control strain, as auxotrophies can impact secondary metabolite production. This procedure allowed assignment of causal loci in the MRB mutants as previously characterized and uncharacterized as described below.

MRB strains that had mutations in genes known to impact ST biosynthesis. (i) MRB283-*laeA*, MRB298-*laeA*, MRB333-*laeA*, MRB346-*laeA*, and MRB357-*laeA*. Five strains were found to contain mutations in *laeA*, and complementation with a wild-type *laeA* allele led to at least partial restoration of NOR production (Fig. 1A). Four of these strains had nonsynonymous mutations, while one (MRB333) had a 29-bp deletion that led to a frameshift and subsequent generation of a premature stop codon (Table 1; Table S1). The amino acids substituted in the point mutants are highly conserved in other characterized LaeA proteins from multiple genera (Fig. S3). Consistent with previous studies on the first characterized mutated *laeA* allele (MRB300) (16), we detected a reduction in *aflR* expression in other MRB-*laeA* mutants (Fig. 1A). In summary, of the 23 MRB mutants isolated, six contained mutations in *laeA*.
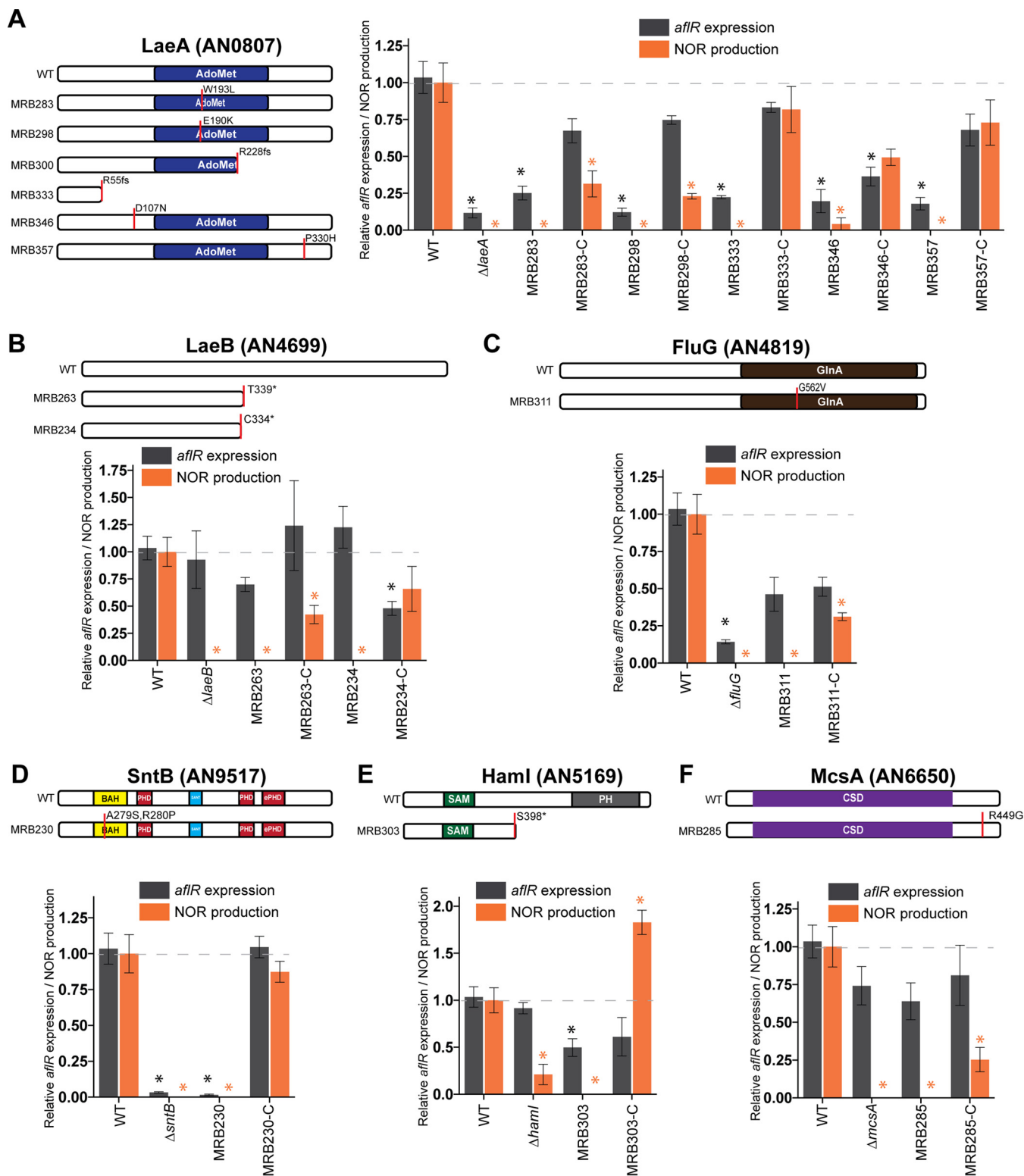
FIG 1 NOR production and *aflR* expression in deletion and point mutants. NOR production was quantified via HPLC analysis of cultures grown on oatmeal medium agar plates, while *aflR* expression was quantified via qPCR analysis of cultures grown in GMM liquid shake cultures. Both NOR production and *aflR* expression were normalized to wild-type levels. Each gene identified from the screen has its own panel (A-F), which includes a schematic of conserved protein domains and graph of the respective deletion, point mutant, and complemented strain. For each sequenced strain, a schematic of the protein is shown with the identified mutation marked. In panel A, the classically characterized MRB300 is included in the protein model for reference (16). Asterisks in the figure represent statistically significant differences ($P < 0.05$) from wild-type results that were calculated using ANOVA in all the combined data, and multiple comparisons were done using Dunnet's test. Abbreviations: AdoMet, *S*-adenosyl methionine binding site; GlnA, glutamine synthetase domain; BAH, bromo-adjacent domain; SANT, "Swi3, Ada2, N-Cor, and TFIIIB"; PHD, plant homeodomain finger; ePHD, extended plant homeodomain finger; SAM, sterile alpha motif; PH, pleckstrin homology domain; CSD, citrate synthase family domain.

(ii) MRB285-*mcsA*. MRB285, the sixth MRB mutant to contain mutations in *mcsA*, was partially restored for NOR production with a wild-type *mcsA* allele (Fig. 1F). Similarly to *laeA*, *mcsA* was originally found by classical mapping approaches and by construction of diploids with other MRB mutants (15). As mentioned earlier, the presence of loss-of-function *mcsA* alleles leads to increased pools of propionyl-CoA, which blocks the synthesis of several polyketides, including ST (15), as evidenced by the loss of NOR production in the *mcsA* deletion and point mutants. However, loss of *mcsA* does not affect expression of the ST cluster transcriptional regulator *aflR*, as *aflR* expression was not reduced in either the Δ*mcsA* strain or the original point mutant (Fig. 1F).

(iii) MRB265-*stcA*. Although the original screen was crafted to exclude genes linked to the ST cluster, we nevertheless found that MRB265 contained a mutation in *stcA*. *stcA* encodes the polyketide synthase required to synthesize the ST backbone, and a previous study had demonstrated that deletion of this gene (originally called *pksST*) eliminated ST synthesis (39). Once the *stcA* mutation was found, further work on this strain ceased.

(iv) MRB311-*fluG*. *fluG* encodes a developmental regulator containing a glutamine synthetase domain that is required for both asexual sporulation and ST production (38, 40). FluG does not function in glutamine biosynthesis but instead synthesizes an extracellular signal that is required for proper asexual development and ST biosynthesis (40, 41). Loss of *fluG* leads to reduction, but not elimination, of aflatoxin production in *A. flavus* (42). Consistently, we observed a reduction in NOR production from the Δ*fluG* mutant as well as the *fluG* point mutant (MRB311), and complementation of *fluG* resulted in partial restoration of NOR production. While *fluG* has not been previously identified as being involved in *aflR* expression, we detected a reduction in *aflR* expression in the Δ*fluG* mutant; however, there was no statistically significant reduction in *aflR* expression in the MRB311 point mutant (Fig. 1C).

Restoration of NOR production in MRB strains by complementation with uncharacterized genes. (i) MRB303 AN5169-*hamI*. The AN5169 protein shares 30% percent identity with the Ham-9 protein described in *Neurospora crassa*. Conforming to *A. nidulans* genetic nomenclature, we refer to it as HamI (43). Ham-9 appears to regulate cross-communication of the mitogen-activated protein kinase (MAPK) pathways in *N. crassa* and is required for hyphal fusion (43). The *hamI* gene encodes an 858-amino-acid (aa) protein containing two conserved domains: a sterile alpha motif (SAM), which is a potential protein-protein interaction domain in scaffold proteins, and a pleckstrin homology-like (PH) domain, which is typically responsible for targeting a protein to the appropriate cellular location (Fig. 1E) (43, 74, 75). Deletion of *hamI* results in reduction, but not elimination, of NOR production, while complementation of the *hamI* point mutant results in an increase in NOR production (Fig. 1E). NOR production is independent of ST cluster transcriptional regulation as *aflR* is expressed at wild-type levels in the deletion mutant (Fig. 1E).

(ii) MRB234 and MRB263 AN4699-*laeB*. MRB234 represents one of the original MRB mutants that resulted in a loss of *aflR* expression (14). We have found that growth conditions influence *aflR* expression in a Δ*laeB* (loss of *aflR* expression) strain, as neither the deletion strain nor MRB234 nor MRB263 showed a loss of *aflR* expression in a liquid shake assay (Fig. 1B). However, *aflR* expression in the Δ*laeB* strain was lost during the induction of asexual development (Fig. S4), and the growth conditions described by Butchko et al. (14) also resulted in loss of *aflR* expression in MRB234. With an absence of characterized homologs, AN4699 is named for this loss-of-*aflR*-expression phenotype. *laeB* encodes a 767-aa protein, with weak homology to G-protein pathway suppressor and transcription initiation factor IIA (TFIIA) domains. This gene represents an unknown pathway that may regulate ST production transcriptionally as well as through downstream processes.

(iii) MRB230 AN9517-*sntB*. MRB230 was previously called *laeC* by Butchko et al. (14); however, AN9517 is a homolog of the yeast gene *SNT2* (E3 ubiquitin ligase), which coordinates the transcriptional response to hydrogen peroxide stress (44, 45). A ho-

molog in the plant pathogen *Fusarium oxysporum*, Snt2, is required for full pathogenicity on muskmelon (46). Thus, we refer to AN9517 as *sntB* in accordance with *Aspergillus* naming conventions. There were two mutations found in *sntB*, both of which are located in a bromo-adjacent homology (BAH) domain which can act as a protein-protein interaction module (47), as well as interacting directly with histones (48, 49). These mutations most likely eliminate an interaction that is required for *aflR* expression. Indeed, both *aflR* expression and NOR production are drastically reduced in both the Δ*sntB* strain and the *sntB* point mutant, while complementation of MRB230 results in full restoration of *aflR* expression as well as NOR production (Fig. 1D).

MRB mutants without identified causative loci. (i) MRB320. This strain contained only one mutation in an open reading frame, located in AN1932 (*msrB*). MsrB is an enzyme belonging to a specific class of methionine (Met) sulfoxide reductases, able to reduce protein-bound methionine sulfoxide to methionine bound in the *R*-form (50–52). Deletion of *msrB* did not reduce NOR accumulation as assessed by eye on oatmeal media (data not shown). Considering that the original screen used a strain with a *metG1* auxotrophy and that supplementation of methionine into culture medium is partially suppressive with respect to ST production (data not shown), we explored the possibility that the presence of mutations in two genes (*metG1* and *msrB*) involved in the biosynthesis and regulation of methionine in a strain could explain the loss of NOR production in the original MRB320 mutant. Therefore, we constructed a double mutant strain (Δ*msrB metG1*) and assayed its ability to accumulate NOR. NOR production levels in this mutant did not differ significantly from wild-type levels (Fig. S5).

(ii) MRB369. MRB369 contained sequence variants in five genes; however, NOR production was not reduced in any of the single-gene-deletion strains. Similarly to MRB320, one of the variants was in a gene (AN7034) predicted to be involved in methionine biosynthesis and homologous to *methionine requiring22* (*MET22*) in yeast. However, a knockout of AN7034 constructed in a *metG1* background showed no significant difference in the level of NOR production from the wild-type level (Fig. S5). The causal mutation was not found in MRB369.

(iii) MRB327 and MRB365. There were four genes with sequence variants in strain MRB327 and five genes in MRB365 with variants (Table 1; Table S1). Single gene deletions in these nine loci did not affect NOR production using the oatmeal assay method (data not shown), so we could not determine the variant responsible for the loss of the NOR phenotype.

(iv) MRB326. No mutations were found in predicted open reading frames in MRB326, nor did the structural variant analysis identify a credible variant.

Global secondary metabolite regulation mutants. To test if deletion of any of the newly identified transcriptional regulators of *aflR*, *laeB*, or *sntB* had an impact on other BGC products in addition to ST, we analyzed the metabolome of the Δ*laeB*, Δ*sntB*, and Δ*laeA* strains using liquid chromatography coupled with mass spectrometry (LCMS). We compared each deletion mutant to a wild-type control (BTP69) which arose from the same cross as the deletion parent strain. Following data collection, the XCMS package in R was used for feature detection and quantification of the relative levels of the metabolites in each sample (53). We then compared the metabolites that were significantly upregulated or downregulated (fold change greater than 2; *P* value of 0.05 or less) to a list of known secondary metabolites from *A. nidulans* recorded in the Reaxys database. Using an allowed mass error of 5.0 ppm, we generated a list of putative known secondary metabolites from *A. nidulans* whose levels were significantly increased or decreased in the deletion mutants (Table 2; Table S2). These putative metabolite matches help to explain a fraction of the variance for some of these strains and also suggest that *laeB* and *sntB* may act in larger transcriptional networks and are not ST specific (Table 2). The putative known secondary metabolite matches in the Δ*laeB* and Δ*sntB* mutants differ in number and identity, which could imply that these two transcriptional regulators may work in different networks and intersect only with respect to ST and austinol regulation (Table 2).

TABLE 2 Putative known metabolites differentially regulated in transcriptional mutants[a]

Gene deletion	Cluster backbone corresponding to metabolite (name)	Class of backbone	Final product of cluster	Change(s) in abundance
laeA	ANID_08383 (ausA)	PKS	Austinol	Both
	ANID_07909 (orsA)	PKS	F-9775	Increase
laeB	ANID_08383 (ausA)	PKS	Austinol	Both
sntB	ANID_08383 (ausA)	PKS	Austinol	Both
	ANID_07909 (orsA)	PKS	F-9775	Increase
	ANID_08209 (wA)	PKS	Conidial pigment	Increase
	ANID_00150 (mdpG)	PKS	Monodictyphenone	Increase
	ANID_06448 (pkbA)	PKS	Cichorine	Decrease
	ANID_03396 (micA)	NRPS	Microperfuranone	Decrease
	ANID_07071 (pkgA)	PKS	Alternariol	Decrease

[a]Data represent putative matches of known *A. nidulans* secondary metabolites, based on exact mass, from deletion mutants that regulate the ST gene cluster transcriptionally. The major synthase that produces the matched compound is listed, followed by the class of enzyme and the final product of that secondary metabolite cluster. The change of abundance is listed in comparison to the abundance in the wild type. Both, increase plus decrease. Detailed information on the observed metabolite matches is provided in Table S2. PKS, polyketide synthase; NRPS, nonribosomal peptide synthetase.

Novel regulators of ST are required for aflatoxin production in *A. flavus*. The initial goal of the 1999 study by Butchko et al. was to identify aflatoxin regulators by using *A. nidulans* as a model. Upon the identification of three uncharacterized genes in *A. nidulans*, we proceeded to delete these genes in *A. flavus* and to assess the impact on aflatoxin production. Homologs were identified using BLAST analysis of *laeB* (AFLA_099790), *sntB* (AFLA_029990), and *hamI* (AFLA_021920) (54). These genes were deleted in the NRRL3357 background and were confirmed via Southern blotting (Fig. S6). To assess the impact on aflatoxin production, strains were point inoculated on glucose minimal media (GMM). A *laeA* deletion strain was grown simultaneously as a control for loss of aflatoxin. Aflatoxin production was decreased in each of the deletion strains generated (Fig. 2). This illustrates that these genes from *A. nidulans* have a conserved role and also demonstrates the success of our screen in identifying regulators of aflatoxin.

DISCUSSION

The advent of well-annotated reference genomes in fungal biology has spawned an era of reverse genetics where genes and pathways have been extensively studied in a fungus because orthologs in different species may have had some potential link to an interesting phenotype. While this research approach has been interesting and fruitful,
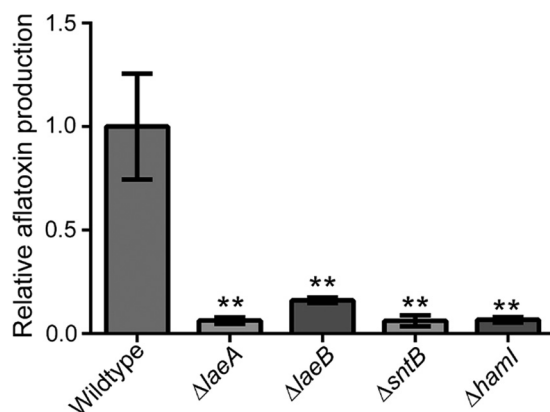

FIG 2 Gene deletions of novel regulators in *A. flavus* lead to a loss of aflatoxin production. Aflatoxin production was assessed on solid GMM plates, and levels are shown relative to wild-type levels (NRRL3357). Aflatoxin production was lost in strains where *laeA*, *laeB*, *sntB*, or *hamI* was deleted. Each strain was grown in triplicate. Asterisks indicate statistical significance ($P < 0.005$) calculated using an unpaired t test.

few fungal genes display conserved phenotypes between species, even those species that are considered closely related. The power of forward genetic screening lies in the unbiased approach of finding genes involved with a biological process and, specifically, the ability to genetically track a phenotype. However, identifying and characterizing mutants through genetic screens have historically been challenging. Difficulties include the inability to map the mutation (reliant on a well-established Mendelian system and good coverage with known markers) or to genetically complement the mutation with a full-coverage DNA library. With the relatively small size of most fungal genomes and the continually declining price of whole-genome sequencing, there is now an opportunity for the revitalization of forward genetic screening for identifying and characterization of novel genetic pathways. Next-generation sequencing represents a solution to old genetic problems and can be used to move the field toward a more complete picture of gene regulation, biochemistry, and cellular biology (31, 55, 56).

The use of Ion Torrent and Illumina sequencing technology allowed us to generate whole-genome sequences and successfully identify the causative mutations in 12 of the 17 isolates that we sequenced. Rapid gene deletion in *A. nidulans* further enhanced our ability to quickly confirm the sequencing data. Notably, there are five mutants for which we have been unsuccessful in identifying mutations (MRB320, MRB326, MRB327, MRB365, and MRB369), which could have been due to the presence of noncoding mutations in regulatory regions, as there are valid variants in noncoding regions in several of these MRB strains. However, considerable effort would need to be expended to experimentally validate the effects of these variants. Alternatively, the phenotype may be a result of multiple variants leading to the loss of the NOR phenotype seen in MRB327 and MRB365 and could explain why single gene knockouts do not restore this phenotype in an independent genetic background. The initial analysis in the work described by Butchko et al. (14) attempted to assign linkage groups based on frequencies of recombination between mutants; however, it is clear from the data that this approach was only partially successful, as additional mutations in both *laeA* (five more mutant alleles) and *mcsA* (one additional mutant allele) were discovered through sequencing (14).

Interestingly, of the original 23 MRB mutant strains, approximately 50% turned out to harbor mutations in *laeA* or *mcsA*. Perhaps part of this bias is a result of how the genetic screen was designed, which relied on visual identification of NOR and discarded mutants with extreme developmental phenotypes. This is important for interpretation of these results, as one would expect that a saturated genetic screen would have also discovered additional genes in the velvet complex (VeA and VelB). However, it is understandable that mutations in *veA* or *velB* would have been missed in a visual screen due to the presence of increased levels of orsellinic acid produced by these mutants, which makes the strains look very dark in color and masks NOR pigmentation (57). Consistently, deletions of both *laeA* and *mcsA* result in loss of ST in addition to other pigments produced by the fungus, thereby making the mutants more easily distinguishable in a visual NOR screen. Regardless, due to the rediscovery of additional *laeA* mutants in the screen, we now have more information on which residues are required for proper LaeA function. Two mutations, E190K and W193L, map to the conserved methyltransferase protein domain and may disrupt the protein binding *S*-adenosyl methionine. The exact role played by the two additional mutated residues (D107 and P330) is unknown as they are located outside the conserved adenosyl methionine (Ado-Met) domain but are highly conserved in other LaeA homologs (see Fig. S3 in the supplemental material). Further study of these mutations may assist in our understanding of the mechanistic role that the enigmatic LaeA protein plays in fungal cellular biology.

In addition to *laeA* and *mcsA*, the screen identified several genes that were not previously known to be involved in regulation of the biosynthesis of ST. One example is the *N. crassa ham-9* homolog that we term *hamI* (AN5169). In *N. crassa*, HAM proteins are involved with cell-to-cell fusion or hyphal anastomosis, which is a requirement for asexual and sexual development (43). Several studies have shown that *Aspergillus*
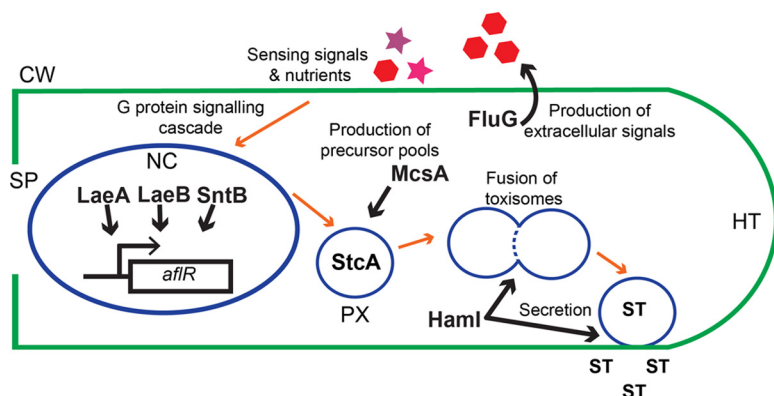
FIG 3 Placement of MRB proteins in sterigmatocystin biosynthesis. The figure shows a schematic of a fungal hypha, the predicted or known location and function of each protein that was identified from the MRB screen, and their proposed role in ST production. ST production requires orchestration of many cellular processes, starting with the production (FluG) and perception of extracellular signals (41). Signal transduction pathways sensing extracellular signals, such as G protein-coupled receptors, initiate a signaling cascade that feeds into the nucleus (NC) where LaeA, LaeB, and SntB are required for transcription of *aflR*, the transcriptional regulator of the ST BGC (10). Following transcription of the required ST biosynthetic machinery, ST synthesis is initiated in the peroxisome (73), requiring availability of proper precursor pools, which relies in part on the presence of McsA (15). ST synthesis progresses through fusion of small vesicles, facilitated by HamI, to form toxisomes containing the end metabolite which is secreted to the environment. Features of the fungal cell are abbreviated as follows: CW, cell wall; SP, septum; NC, nucleus; PX, peroxisome; HT, hyphal tip.

utilizes the endomembrane system for production and transport of the "aflatoxisomes" that function to compartmentalize several of the enzymatic steps leading to production of this toxin (58, 59). In the aspergilli, HamI could be required for the correct fusion of vesicles to vacuoles or the plasma membrane to properly synthesize and export secondary metabolites such as NOR and ST. Consistent with this hypothesis, HamI operates downstream of the ST BGC as *aflR* is expressed at wild-type levels in these genetic backgrounds.

We were also able to identify two novel transcriptional regulators of the ST BGC, *laeB* (AN4699) and *sntB* (AN9517). The LaeB protein is predicted to contain two domains with low homology: a G-protein pathway suppressor domain and a transcription initiation factor IIA (TFIIA) domain. Growth conditions appear to play a role in the way LaeB regulates ST (Fig. 1B) (Fig. S4), as LaeB seems to regulate ST production transcriptionally as well as potentially through another unidentified pathway. Regarding SntB, the predicted gene model appears to be incorrect in the NCBI database as well as on the Aspergillus Genome Database (60, 61). Both databases predict the presence of gene products smaller than the SNT2 homolog in *Saccharomyces cerevisiae*, *A. fumigatus*, and *A. flavus*. SNT2 is an E3 ubiquitin ligase that has been shown to localize to promoters of stress response genes and is involved in the ubiquitination and degradation of excess histones (44, 45). SNT2 is observed to associate with histone-modifying enzymes in fission and budding yeasts (62). In *F. oxysporum* and *N. crassa*, Snt2 mutants are impaired in reproduction (as well as in pathogenicity on muskmelon in the case of *F. oxysporum*) (46). SNT2 contains the BAH domain as well as a SANT domain and three plant homeodomain (PHD) fingers that interact with histone H3 in yeast (45). Our current hypothesis is that SntB regulates ST through chromatin remodeling, a regulatory process previously shown to control ST and many other secondary metabolite gene clusters (63–67).

Our current knowledge of ST biosynthesis and regulation paints a picture of a multitiered regulatory system (Fig. 3). A prerequisite for production of secondary metabolites is the availability of appropriate precursor pools. In concert with precursor availability, external environmental stimuli are sensed, which elicits a downstream transcriptional response. Starting with transcriptional regulators and chromatin remodelers, there is complex communication between several networks to properly activate

a BGC. Gene clusters that are transcriptionally silent during primary growth may require alterations in chromatin structure. The activity of the velvet complex is one way in which environmental stimuli give rise to chromatin remodeling while at the same time inducing expression of cluster-specific transcription factors (23). Cluster-specific transcription factors in turn activate biosynthetic enzymes that are responsible for synthesis of the metabolite. Cellular machinery is required for small-molecule assembly and eventual transport. Thus, regulation of the BGCs can be enhanced or disrupted at many different junctures in the fungal cell. Following transcription, the precursor pools of starting material and compartmentalization of the cell require precise movement and shuttling to protect the cell and to properly synthesize the final product.

By using whole-genome sequencing and Mendelian crosses to characterize mutants from a genetic screen, this work has addressed gaps in the complex process of fungal secondary metabolism, including the identification of players in several cellular processes that were not previously known to influence secondary metabolism. There were three transcriptional regulators identified that are required for *aflR* expression (LaeA, LaeB, and SntB), and, lastly, a protein was identified that may have a role in toxisome fusion (HamI). Moreover, we have successfully demonstrated once more the advantages of using a facile genetic model, *A. nidulans*, to identify mycotoxin regulatory genes in the agricultural pathogen *A. flavus*. We anticipate that these novel regulators and pathways influencing aflatoxin/ST production will not only expand our understanding of the cellular machinery required for mycotoxin synthesis but also inspire a return to forward genetics.

MATERIALS AND METHODS

Culture conditions. Strains used in this study are listed in Table S3 in the supplemental material and were grown on glucose minimal media (GMM) with additional supplements for auxotrophic strains (68). These strains were maintained as glycerol stocks stored at $-80°C$.

Sexual crossing and backcrosses. TJH3.40 and RJMP1.1 were crossed to generate progenies RAAS233.2, which was used as the parental strain to construct deletion mutants, and RBTP69, which was used as an isogenic control for these deletion mutants. To combine the gene deletions with a *metG1* mutation, TXL21 and TXL22 were crossed with TJH3.40 to generate TXL23 and TXL24, respectively. MRB mutants were backcrossed to RJW2, and progeny that were methionine or biotin auxotrophs and could not produce NOR were selected for subsequent backcrosses and sequencing.

Next generation sequencing and SNP detection. Each MRB strain was backcrossed to the same strain (RJW2) two to seven times and genomic DNA was extracted from each isolate (31). Two independent isolates of MRB234 were sequenced on the Illumina GAIIx platform at the University of Wisconsin Biotechnology Center. MRB234 variants were detected as previously described (31). The remaining 16 MRB mutants and a nearly isogenic wild-type control were sequenced on an Ion Torrent Personal Genome Machine (PGM). Ion Torrent-compatible 400-bp sequencing libraries were constructed using an Ion Plus fragment library kit (catalog no. 4471252), and unique barcodes from an Ion Xpress Barcode adapter kit (catalog no. 4474518) were used for multiplex sequencing. Libraries were combined equally in sets of 4 and were templated using an Ion PGM Template OT2 kit (catalog no. 4479882), loaded onto a 318v2 sequencing chip (catalog no. 4484354), and sequenced using an Ion 400-bp sequencing kit (catalog no. 4482002). Sequencing reads were processed using the Ion Torrent Server Suite (v4.0.2) with the default settings. Data were then imported into CLC Genomics Workbench v8.0.2 for variant detection. Reads were first quality trimmed using the "Trim Sequences" tool (trim_5'=6, trim_ambiguous=2, quality_trim=0.05) and aligned to the *A. nidulans* FGSCA4 reference genome (http://www.aspgd.org [version s10-m04-r06]) using the "Map Reads to Reference" (default settings) tool, and the alignment was further refined around insertions/deletions using the "Local Realignment" tool. Variants were detected in the mapping data using the "Basic Variant Detection" tool (ploidy=1, min_cov=4, min_count=2, min_freq=75.0, base_quality_filter=on, remove_pyro_errors=on). Variants for each isolate were then filtered using the "Filter against Known Variants" tool with all the other isolates as a variant database. The filtered variants were then passed through the "Amino Acid Changes" tool to filter out nonsynonymous substitutions, and then, finally, insertion/deletion variants were removed. For all variants that remained, the mapping data were manually inspected to confirm that the variant was present in the raw data. For mutants where this workflow did not yield any validated SNPs, the mapping data were then analyzed for structural variants using the "InDels Structural Variant" tool followed by the "Amino Acid Changes" tool.

Validation of mutations through gene deletion and complementation. Double-joint PCR was used to construct deletion mutants TBTP45-52 and TXL21-22 (Table S3) using oligonucleotides listed in Table S4 (69). Briefly, 1 to 2 kb of 5' and 3' flanking sequence of each gene of interest was amplified using oligonucleotides listed in Table S3 (i.e., 5'-F paired with 5'-R) from RAAS233.2 genomic DNA, with the *pyrG* marker amplified from genomic DNA isolated from *A. fumigatus*. These fragments were then fused together via PCR to generate deletion constructs. RAAS233.2 was then transformed with these con-

structs, and successful deletion of gene of interest was confirmed by Southern blot analysis. The 5' and 3' fragments used in the double-joint PCR were used as probes labeled with dCTP α-P^{32}.

Backcrossed and sequenced strains were transformed with plasmids containing a full wild-type copy of the gene suspected to be the cause of the loss of the NOR phenotype as well as a selectable marker (either *metG* or *biA*). Complementation of MRB283, MRB298, MRB333, MRB346, and MRB357 was performed with pBTP7. pBTP7 was constructed by freeing a 3.0-kb fragment containing *laeA* from pJW45-4 (16) with HindIII and cloning this fragment in HindIII-linearized pUG11-41 (70). MRB285 was complemented with pBTP6, which was constructed by amplifying a 2.8-kb fragment containing *mcsA* using BP AN6650-F/BP AN6650-R (Table S2), digested with HindIII, and cloned into linearized pUG11-41. MRB303 was complemented with pJMP248.3, which was constructed by amplifying *ham9* with JP AN5169 For(HindIII)/JP AN5169 Rev(HindIII), digested with HindIII, and cloned into linearized pUG11-41. MRB311 was complemented with pJMP249.1, which was constructed by amplifying *fluG* with JP AN4819 For(HindIII)/JP AN4819 Rev(HindIII), digested with HindIII, and cloned into linearized pUG11-41. pBTP8 was constructed using homologous recombination in yeast using an adapted protocol (71) and was assembled by amplifying *laeB* using primers BP AN4699-F-YS/BP AN4699-R-YS, as well as by amplifying *metG* using primers BP metG F YS/BP metG R YS, and these were combined with pYHC-wA-pyrG that had been linearized and were used in a yeast transformation. MRB230 was complemented with pBTP9, which was assembled using homologous recombination in yeast as well. For pBTP9, *sntB* was amplified using BP AN9517 comp F/BP AN9517 comp R and *biA* was amplified using BP biA/9517 F YS/BP biA rev YS, and these were combined with linearized pYHC-wA-pyrG in a yeast transformation. To bring strains to prototrophy, all strains, aside from MRB230, were transformed with pUG11-41. MRB230 was brought to prototrophy using BTP10, which was assembled using homologous recombination in yeast as well by the use of amplified *biA* with primers BP biA fwd YS/BP biA rev YS and linearized pYHC-wA-pyrG in a yeast transformation.

Generation of *A. flavus* deletion mutants. Double-joint PCR was used to construct deletion cassettes to delete *laeB*, *sntB*, and *hamI*. *laeB* was deleted in NRRL3357.5, and the result was confirmed by Southern blotting (Fig. S3). *sntB* was deleted in TXZ21.3, which is a *pyrG* and *argB* auxotrophic strain with KU70 deleted to promote homologous recombination. To construct this strain, we deleted the *argB* gene with a copy of *pyrG* in TJES19.1 (Zhao, Keller, et al., unpublished) to make TJES20.1, an arginine auxotroph. *pyrG* was then deleted in a transformation using primers in Table S3 to generate TXZ21.3. Gene deletions in XZ21.3 were performed using *argB* as a selectable marker, and then a copy of *pyrG* from *A. fumigatus* was placed at the KU locus to bring the strains to prototrophy. Lastly, *hamI* was deleted by replacing the open reading frame with a copy of *pyrG* from *A. fumigatus* in TJES19.1, resulting in TXZ1.2. These genetic manipulations were confirmed by Southern blot analysis (Fig. S6).

Quantification of *aflR* expression. For quantitative PCR (qPCR), strains were grown in liquid GMM supplemented with pyridoxine at a concentration of 1.0×10^6 spores/ml and with shaking at 250 rotations/min at 37°C for 72 h. Mycelia were harvested by filtering through Miracloth (CalBioChem) and were lyophilized. Total RNA was then isolated using Trizol (Invitrogen). A 1-μg volume of total RNA was digested with DNase I (New England Biolabs), and cDNA was synthesized using an iScript kit (Bio-Rad). A TaqMan qPCR assay was designed for actin (*actA*) and was composed of a dually labeled probe, 5' CAL Fluor gold 540-CGGTGGTTCCATCTTGGCTTCTC-black hole quencher (BHQ)-3' (LGC BioSearch), and primers Anid_actA_F/Anid_actA_R. *aflR* was assayed using a dually labeled probe, 5'-6-carboxyfluorescein (FAM)-CTGCCTGTCCATCTGCCTGGA-BHQ-3' (LGC BioSearch), and primer pair Anid_aflR_F/Anid_aflR_R. TaqMan qPCR assays were conducted according to the recommendations of the manufacturer using a TaqMan Universal qPCR kit (Thermo Fisher) and an ABI Step One Plus qPCR machine (Thermo Fisher). Relative quantification data were calculated for *aflR* using the threshold cycle ($\Delta\Delta C_T$) method with actin as an internal control and normalization to the wild type (RBTP69) (72). Statistical significance was measured using analysis of variance (ANOVA) in GraphPad Prism v6, and comparisons to the wild type were done using Dunnett's test.

For Northern analysis, strains were grown in liquid GMM at a concentration of 1.0×10^6 spores/ml with shaking at 250 rotations/min at 37°C for 24 h. Mycelia were harvested by filtration through Miracloth (CalBioChem) and were transferred to solid GMM for 24 h. Tissue was lyophilized, and total RNA was then isolated using Trizol (Invitrogen). The probe for *aflR* was prepared by PCR amplification of genomic DNA (Table S2) and was labeled with dCTP α-P^{32}.

Secondary metabolite analysis. For NOR analysis, visualization of NOR for screening purposes was performed on solid 1% oatmeal media with appropriate supplements at 37°C after 3 days. To measure and quantify NOR, strains were point inoculated on 1% oatmeal media, and a 1.0-cm core was taken from the plate after 3 days of growth. This core was first homogenized in 3 ml of 0.01% Tween 20 and then extracted with 3 ml of ethyl acetate. Samples were shaken and spun for 10 min at 3,000 rpm. The organic layer was removed, dried, and resuspended in 100% acetonitrile (ACN). Samples were filtered through an Acrodisc syringe filter with a nylon membrane (Pall Corporation) (0.45-μm pore size). The samples were run on a PerkinElmer Flexar instrument equipped with a Zorbax Eclipse XDB-C$_{18}$ column (Agilent) (150 mm long; 4.6-mm inner diameter; 5 μm pore size). The column was equilibrated in 70% solvent B (acetonitrile with 1.0% formic acid) and 30% solvent A (water with 1% formic acid) for 3 min. With a flow rate of 1.8 ml per min, the column went from 70% to 100% solvent B for 10 min to 100% solvent B for 2 min and then back to 70% solvent B for 3 min. NOR was detected by a photo diode array (PDA) detector (PerkinElmer) set to 485 nm with a reference wavelength of 600 nm.

For aflatoxin analysis, 10^3 spores were point inoculated on solid GMM plates and incubated at 29°C for 7 days in the dark. Samples were prepared in a fashion similar to that described above and were resuspended in 20% acetonitrile–1% formic acid and filtered as described above. Samples were

separated on a Zorbax Eclipse XDB-C$_{18}$ column (Agilent) (4.6 mm by 150 mm, 5-μm particle size) by using a binary gradient of 1% (vol/vol) formic acid as solvent A and acetonitrile with 1% formic acid as solvent B. Aflatoxin was detected using a Flexar fluorescence light (FL) detector (PerkinElmer) with the excitation wavelength set to 365 nm and the emission wavelength set to 455 nm. The binary gradient started with an isocratic step at 80% solvent A for 1 min followed by a linear gradient to 35% solvent A in 10 min and an additional linear gradient to 100% solvent B for 0.5 min with a flow rate of 1.5 ml/min.

For MS sample preparation, 10^3 spores were point inoculated on solid GMM-pyridoxine plates and were incubated at 37°C for 5 days. Samples had a 1.0-cm core removed that was subsequently homogenized in 3.0 ml of Tween 20. Metabolites were extracted with 3.0 ml of ethyl acetate, shaken vigorously, and spun down at 3,000 rpm for 10 min. The organic layer was removed and dried. Samples were resuspended in 20% acetonitrile and filtered through an Acrodisc syringe filter with nylon membrane (Pall Corporation) (0.45 μm pore size). High-resolution ultra-high-performance liquid chromatography–mass spectrometry (UHPLC-MS) was performed on a Thermo Scientific-Vanquish UHPLC system connected to a Thermo Scientific Q Exactive Orbitrap operated in electrospray negative-ionization mode (ESI$^-$). A Zorbax Eclipse XDB-C$_{18}$ column (2.1 by 150 mm, 1.8-μm particle size) was used with a flow rate of 0.2 ml per min for all samples. The solvent system was water with 0.5% formic acid (solvent A) and acetonitrile with 0.5% formic acid (solvent B) with the following gradient: 20% to 100% solvent B from 0 to 15 min, 100% solvent B from 15 to 20 min, 100% to 20% solvent B from 20 to 21 min, and 20% solvent B from 21 to 25 min. Nitrogen was used as the sheath gas. Data acquisition and processing for the UHPLC/MS were controlled by Thermo Scientific Xcalibur software. Files were converted to the .mzXML format using MassMatrix MS Data File Conversion, grouped by condition, and run in the XCMS package in R (53). Differential masses found via XCMS were filtered using criteria consisting of a fold change greater than 2 and a P value below 0.05. These were then compared to a list of known secondary metabolites downloaded from the Reaxys database (version 2.20770.1; Elsevier Information Systems GmbH, Frankfurt, Germany). Peak identification occurred if the observed m/z value matched the predicted m/z value with no more than a 5.0-ppm error. Parts-per-million error values were calculated by dividing the mass error by the exact mass and multiplying the result by 10^6.

Accession number(s). Sequencing data are available through NCBI SRA database accession no. SRP098130 and BioProject database accession no. PRJNA369071.

SUPPLEMENTAL MATERIAL

Supplemental material for this article may be found at https://doi.org/10.1128/mBio .01246-17.

FIG S1, TIF file, 4.6 MB.

FIG S2, TIF file, 19.3 MB.

FIG S3, TIF file, 17.9 MB.

FIG S4, TIF file, 1.6 MB.

FIG S5, TIF file, 0.02 MB.

FIG S6, TIF file, 0.3 MB.

TABLE S1, DOCX file, 0.02 MB.

TABLE S2, DOCX file, 0.02 MB.

TABLE S3, DOCX file, 0.02 MB.

TABLE S4, DOCX file, 0.02 MB.

REFERENCES

1. Amare MG, Keller NP. 2014. Molecular mechanisms of *Aspergillus flavus* secondary metabolism and development. Fungal Genet Biol 66:11–18. https://doi.org/10.1016/j.fgb.2014.02.008.

2. Yu J. 2012. Current understanding on aflatoxin biosynthesis and future perspective in reducing aflatoxin contamination. Toxins 4:1024–1057. https://doi.org/10.3390/toxins4111024.

3. Georgianna DR, Payne GA. 2009. Genetic regulation of aflatoxin biosynthesis: from gene to genome. Fungal Genet Biol 46:113–125. https://doi.org/10.1016/j.fgb.2008.10.011.

4. Nesbitt BF, O'Kelly J, Sargeant K, Sheridan ANN. 1962. *Aspergillus flavus* and Turkey X disease. Toxic metabolites of *Aspergillus flavus*. Nature 195:1062–1063. https://doi.org/10.1038/1951062a0.

5. Williams JH, Phillips TD, Jolly PE, Stiles JK, Jolly CM, Aggarwal D. 2004. Human aflatoxicosis in developing countries: a review of toxicology,

exposure, potential health consequences, and interventions. Am J Clin Nutr 80:1106–1122.

6. Wogan GN. 1992. Aflatoxins as risk factors for hepatocellular carcinoma in humans. Cancer Res 52:2114s–2118s.

7. Keller NP. 2015. Translating biosynthetic gene clusters into fungal armor and weaponry. Nat Chem Biol 11:671–677. https://doi.org/10.1038/nchembio.1897.

8. Keller NP, Adams TH. 1995. Analysis of a mycotoxin gene cluster in Aspergillus nidulans. SAAS Bull Biochem Biotechnol 8:14–21.

9. Chang PK, Cary JW, Bhatnagar D, Cleveland TE, Bennett JW, Linz JE, Woloshuk CP, Payne GA. 1993. Cloning of the Aspergillus parasiticus apa-2 gene associated with the regulation of aflatoxin biosynthesis. Appl Environ Microbiol 59:3273–3279.

10. Woloshuk CP, Foutz KR, Brewer JF, Bhatnagar D, Cleveland TE, Payne GA. 1994. Molecular characterization of aflR, a regulatory locus for aflatoxin biosynthesis. Appl Environ Microbiol 60:2408–2414.

11. Yu JH, Butchko RAE, Fernandes M, Keller NP, Leonard TJ, Adams TH. 1996. Conservation of structure and function of the aflatoxin regulatory gene aflR from Aspergillus nidulans and A. flavus. Curr Genet 29:549–555. https://doi.org/10.1007/BF02426959.

12. van Dijk JWA, Wang CCC. 2016. Heterologous expression of fungal secondary metabolite pathways in the Aspergillus nidulans host system. Methods Enzymol 575:127–142. https://doi.org/10.1016/bs.mie.2016.02.021.

13. Maggio-Hall LA, Hammond TM, Keller NP. 2004. Aspergillus nidulans as a model system to study secondary metabolism, p 197–222. In Romeo JT (ed), Recent advances in phytochemistry, vol 38. Elsevier Ltd. https://doi.org/10.1016/S0079-9920(04)80011-X.

14. Butchko RAE, Adams TH, Keller NP. 1999. Aspergillus nidulans mutants defective in stc gene cluster regulation. Genetics 153:715–720.

15. Zhang YQ, Keller NP. 2004. Blockage of methylcitrate cycle inhibits polyketide production in Aspergillus nidulans. Mol Microbiol 52:541–550. https://doi.org/10.1111/j.1365-2958.2004.03994.x.

16. Bok JW, Keller NP. 2004. LaeA, a regulator of secondary metabolism in Aspergillus spp. Eukaryot Cell 3:527–535. https://doi.org/10.1128/EC.3.2.527-535.2004.

17. Zhang YQ, Brock M, Keller NP. 2004. Connection of propionyl-CoA metabolism to polyketide biosynthesis in Aspergillus nidulans. Genetics 168:785–794. https://doi.org/10.1534/genetics.104.027540.

18. Kale SP, Milde L, Trapp MK, Frisvad JC, Keller NP, Bok JW. 2008. Requirement of LaeA for secondary metabolism and sclerotial production in Aspergillus flavus. Fungal Genet Biol 45:1422–1429. https://doi.org/10.1016/j.fgb.2008.06.009.

19. Jain S, Keller N. 2013. Insights to fungal biology through LaeA sleuthing. Fungal Biol Rev 27:51–59. https://doi.org/10.1016/j.fbr.2013.05.004.

20. Bok JW, Balajee SA, Marr KA, Andes D, Nielsen KF, Frisvad JC, Keller NP. 2005. LaeA, a regulator of morphogenetic fungal virulence factors. Eukaryot Cell 4:1574–1582. https://doi.org/10.1128/EC.4.9.1574-1582.2005.

21. Wiemann P, Brown DW, Kleigrewe K, Bok JW, Keller NP, Humpf HU, Tudzynski B. 2010. FfVel1 and FfLae1, components of a velvet-like complex in Fusarium fujikuroi, affect differentiation, secondary metabolism and virulence. Mol Microbiol 77:972–994. https://doi.org/10.1111/j.1365-2958.2010.07263.x.

22. López-Berges MS, Hera C, Sulyok M, Schäfer K, Capilla J, Guarro J, Di Pietro A. 2013. The velvet complex governs mycotoxin production and virulence of Fusarium oxysporum on plant and mammalian hosts. Mol Microbiol 87:49–65. https://doi.org/10.1111/mmi.12082.

23. Bayram O, Krappmann S, Ni M, Bok JW, Helmstaedt K, Valerius O, Braus-Stromeyer S, Kwon NJ, Keller NP, Yu JH, Braus GH. 2008. VelB/VeA/LaeA complex coordinates light signal with fungal development and secondary metabolism. Science 320:1504–1506. https://doi.org/10.1126/science.1155888.

24. Bayram O, Braus GH. 2012. Coordination of secondary metabolism and development in fungi: the velvet family of regulatory proteins. FEMS Microbiol Rev 36:1–24. https://doi.org/10.1111/j.1574-6976.2011.00285.x.

25. Kato N, Brooks W, Calvo AM. 2003. The expression of sterigmatocystin and penicillin genes in Aspergillus nidulans is controlled by veA, a gene required for sexual development. Eukaryot Cell 2:1178–1186. https://doi.org/10.1128/EC.2.6.1178-1186.2003.

26. Calvo AM, Lohmar JM, Ibarra B, Satterlee T. 2016. Velvet regulation of fungal development, p 475–497. In Growth, differentiation and sexuality. Springer International, Cham, Switzerland.

27. Flibotte S, Edgley ML, Chaudhry I, Taylor J, Neil SE, Rogula A, Zapf R, Hirst

M, Butterfield Y, Jones SJ, Marra MA, Barstead RJ, Moerman DG. 2010. Whole-genome profiling of mutagenesis in Caenorhabditis elegans. Genetics 185:431–441. https://doi.org/10.1534/genetics.110.116616.

28. Puente XS, Pinyol M, Quesada V, Conde L, Ordóñez GR, Villamor N, Escaramis G, Jares P, Beà S, González-Díaz M, Bassaganyas L, Baumann T, Juan M, López-Guerra M, Colomer D, Tubío JMC, López C, Navarro A, Tornador C, Aymerich M, Rozman M, Hernández JM, Puente DA, Freije JMP, Velasco G, Gutiérrez-Fernández A, Costa D, Carrió A, Guijarro S, Enjuanes A, Hernández L, Yagüe J, Nicolás P, Romeo-Casabona CM, Himmelbauer H, Castillo E, Dohm JC, de Sanjosé S, Piris MA, de Alava E, Miguel JS, Royo R, Gelpí JL, Torrents D, Orozco M, Pisano DG, Valencia A, Guigó R, Bayés M, Heath S, Gut M, Klatt P, Marshall J, Raine K, Stebbings LA, Futreal PA, Stratton MR, Campbell PJ, Gut I, López-Guillermo A, Estivill X, Montserrat E, López-Otín C, Campo E. 2011. Whole-genome sequencing identifies recurrent mutations in chronic lymphocytic leukaemia. Nature 475:101–105. https://doi.org/10.1038/nature10113.

29. Schneeberger K, Ossowski S, Lanz C, Juul T, Petersen AH, Nielsen KL, Jørgensen JE, Weigel D, Andersen SU. 2009. SHOREmap: simultaneous mapping and mutation identification by deep sequencing. Nat Methods 6:550–551. https://doi.org/10.1038/nmeth0809-550.

30. Nowrousian M, Teichert I, Masloff S, Kück U. 2012. Whole-genome sequencing of Sordaria macrospora mutants identifies developmental genes. G3 2:261–270. https://doi.org/10.1534/g3.111.001479.

31. Bok JW, Wiemann P, Garvey GS, Lim FY, Haas B, Wortman J, Keller NP. 2014. Illumina identification of RsrA, a conserved C2H2 transcription factor coordinating the NapA mediated oxidative stress signaling pathway in Aspergillus. BMC Genomics 15:1011. https://doi.org/10.1186/1471-2164-15-1011.

32. McCluskey K, Wiest AE, Grigoriev IV, Lipzen A, Martin J, Schackwitz W, Baker SE. 2011. Rediscovery by whole genome sequencing: classical mutations and genome polymorphisms in Neurospora crassa. G3 1:303–316. https://doi.org/10.1534/g3.111.000307.

33. Ohi MD, Link AJ, Ren L, Jennings JL, McDonald WH, Gould KL. 2002. Proteomics analysis reveals stable multiprotein complexes in both fission and budding yeasts containing Myb-related Cdc5p/Cef1p, novel pre-mRNA splicing factors, and snRNAs. Mol Cell Biol 22:2011–2024. https://doi.org/10.1128/MCB.22.7.2011-2024.2002.

34. Irvine DV, Goto DB, Vaughn MW, Nakaseko Y, McCombie WR, Yanagida M, Martienssen R. 2009. Mapping epigenetic mutations in fission yeast using whole-genome next-generation sequencing. Genome Res 19:1077–1083. https://doi.org/10.1101/gr.089318.108.

35. Niu J, Arentshorst M, Nair PDS, Dai Z, Baker SE, Frisvad JC, Nielsen KF, Punt PJ, Ram AFJ. 2015. Identification of a classical mutant in the industrial host Aspergillus niger by systems genetics: LaeA is required for citric acid production and regulates the formation of some secondary metabolites. G3 6:193–204. https://doi.org/10.1534/g3.115.024067.

36. Downes DJ, Chonofsky M, Tan K, Pfannenstiel BT, Reck-Peterson SL, Todd RB. 2014. Characterization of the mutagenic spectrum of 4-nitroquinoline 1-oxide (4-NQO) in Aspergillus nidulans by whole genome sequencing. G3 4:2483–2492. https://doi.org/10.1534/g3.114.014712.

37. Nayak T, Szewczyk E, Oakley CE, Osmani A, Ukil L, Murray SL, Hynes MJ, Osmani SA, Oakley BR. 2006. A versatile and efficient gene-targeting system for Aspergillus nidulans. Genetics 172:1557–1566. https://doi.org/10.1534/genetics.105.052563.

38. Hicks JK, Yu JH, Keller NP, Adams TH. 1997. Aspergillus sporulation and mycotoxin production both require inactivation of the FadA Galpha protein-dependent signaling pathway. EMBO J 16:4916–4923. https://doi.org/10.1093/emboj/16.16.4916.

39. Yu JH, Leonard TJ. 1995. Sterigmatocystin biosynthesis in Aspergillus nidulans requires a novel type I polyketide synthase. J Bacteriol 177:4792–4800. https://doi.org/10.1128/jb.177.16.4792-4800.1995.

40. Lee BN, Adams TH. 1994. The Aspergillus nidulans fluG gene is required for production of an extracellular developmental signal and is related to prokaryotic glutamine synthetase I. Genes Dev 8:641–651. https://doi.org/10.1101/gad.8.6.641.

41. D'Souza CA, Lee BN, Adams TH. 2001. Characterization of the role of the FluG protein in asexual development of Aspergillus nidulans. Genetics 158:1027–1036.

42. Chang PK, Scharfenstein LL, Mack B, Ehrlich KC. 2012. Deletion of the Aspergillus flavus orthologue of A. nidulans fluG reduces conidiation and promotes production of sclerotia but does not abolish aflatoxin biosynthesis. Appl Environ Microbiol 78:7557–7563. https://doi.org/10.1128/AEM.01241-12.

43. Fu C, Ao JJJ, Dettmann A, Seiler S, Free SJ. 2014. Characterization of the

Neurospora crassa cell fusion proteins, HAM-6, HAM-7, HAM-8, HAM-9, HAM-10, AMPH-1 and WHI-2. PLoS One 9:e107773. https://doi.org/10.1371/journal.pone.0107773.

44. Baker LA, Ueberheide BM, Dewell S, Chait BT, Zheng D, Allis CD. 2013. The yeast Snt2 protein coordinates the transcriptional response to hydrogen peroxide-mediated oxidative stress. Mol Cell Biol 33:3735–3748. https://doi.org/10.1128/MCB.00025-13.

45. Singh RK, Gonzalez M, Kabbaj MH, Gunjan A. 2012. Novel E3 ubiquitin ligases that regulate histone protein levels in the budding yeast *Saccharomyces cerevisiae*. PLoS One 7:e36295. https://doi.org/10.1371/journal.pone.0036295.

46. Denisov Y, Freeman S, Yarden O. 2011. Inactivation of Snt2, a BAH/PHD-containing transcription factor, impairs pathogenicity and increases autophagosome abundance in *Fusarium oxysporum*. Mol Plant Pathol 12:449–461. https://doi.org/10.1111/j.1364-3703.2010.00683.x.

47. Callebaut I, Courvalin JC, Mornon JP. 1999. The BAH (bromo-adjacent homology) domain: a link between DNA methylation, replication and transcriptional regulation. FEBS Lett 446:189–193. https://doi.org/10.1016/S0014-5793(99)00132-5.

48. Chambers AL, Pearl LH, Oliver AW, Downs JA. 2013. The BAH domain of Rsc2 is a histone H3 binding domain. Nucleic Acids Res 41:9168–9182. https://doi.org/10.1093/nar/gkt662.

49. Armache KJ, Garlick JD, Canzio D, Narlikar GJ, Kingston RE. 2011. Structural basis of silencing: Sir3 BAH domain in complex with a nucleosome at 3.0 Å resolution. Science 334:977–982. https://doi.org/10.1126/science.1210915.

50. Soriani FM, Kress MR, Fagundes de Gouvêa P, Malavazi I, Savoldi M, Gallmetzer A, Strauss J, Goldman MHS, Goldman GH. 2009. Functional characterization of the *Aspergillus nidulans* methionine sulfoxide reductases (*msrA* and *msrB*). Fungal Genet Biol 46:410–417. https://doi.org/10.1016/j.fgb.2009.01.004.

51. Kim HY, Gladyshev VN. 2007. Methionine sulfoxide reductases: selenoprotein forms and roles in antioxidant protein repair in mammals. Biochem J 407:321–329. https://doi.org/10.1042/BJ20070929.

52. Weissbach H, Resnick L, Brot N. 2005. Methionine sulfoxide reductases: history and cellular role in protecting against oxidative damage. Biochim Biophys Acta 1703:203–212. https://doi.org/10.1016/j.bbapap.2004.10.004.

53. Smith CA, Want EJ, O'Maille G, Abagyan R, Siuzdak G. 2006. XCMS: processing mass spectrometry data for metabolite profiling using nonlinear peak alignment, matching, and identification. Anal Chem 78:779–787. https://doi.org/10.1021/ac051437y.

54. Altschul SF, Gish W, Miller W, Myers EW, Lipman DJ. 1990. Basic local alignment search tool. J Mol Biol 215:403–410. https://doi.org/10.1016/S0022-2836(05)80360-2.

55. Oakley CE, Ahuja M, Sun WW, Entwistle R, Akashi T, Yaegashi J, Guo CJ, Cerqueira GC, Russo Wortman J, Wang CC, Chiang YM, Oakley BR. 2017. Discovery of McrA, a master regulator of Aspergillus secondary metabolism. Mol Microbiol 103:347–365. https://doi.org/10.1111/mmi.13562.

56. Yu Z, Armant O, Fischer R. 2016. Fungi use the SakA (HogA) pathway for phytochrome-dependent light signalling. Nat Microbiol 1:16019. https://doi.org/10.1038/nmicrobiol.2016.19.

57. Bok JW, Soukup AA, Chadwick E, Chiang YM, Wang CCC, Keller NP. 2013. VeA and MvlA repression of the cryptic orsellinic acid gene cluster in *Aspergillus nidulans* involves histone 3 acetylation. Mol Microbiol 89:963–974. https://doi.org/10.1111/mmi.12326.

58. Chanda A, Roze LV, Kang S, Artymovich KA, Hicks GR, Raikhel NV, Calvo AM, Linz JE. 2009. A key role for vesicles in fungal secondary metabolism. Proc Natl Acad Sci U S A 106:19533–19538. https://doi.org/10.1073/pnas.0907416106.

59. Chanda A, Roze LV, Linz JE. 2010. A possible role for exocytosis in aflatoxin export in *Aspergillus parasiticus*. Eukaryot Cell 9:1724–1727. https://doi.org/10.1128/EC.00118-10.

60. NCBI Resource Coordinators. 2016. Database resources of the National Center for Biotechnology Information. Nucleic Acids Res 44:D7–D19. https://doi.org/10.1093/nar/gkv1290.

61. Cerqueira GC, Arnaud MB, Inglis DO, Skrzypek MS, Binkley G, Simison M, Miyasato SR, Binkley J, Orvis J, Shah P, Wymore F, Sherlock G, Wortman JR. 2014. The Aspergillus Genome Database: multispecies curation and incorporation of RNA-Seq data to improve structural gene annotations. Nucleic Acids Res 42:D705–DD710. https://doi.org/10.1093/nar/gkt1029.

62. Roguev A, Shevchenko A, Schaft D, Thomas H, Stewart AF, Shevchenko A. 2004. A comparative analysis of an orthologous proteomic environment in the yeasts *Saccharomyces cerevisiae* and *Schizosaccharomyces pombe*. Mol Cell Proteomics 3:125–132. https://doi.org/10.1074/mcp.M300081-MCP200.

63. Gacek A, Strauss J. 2012. The chromatin code of fungal secondary metabolite gene clusters. Appl Microbiol Biotechnol 95:1389–1404. https://doi.org/10.1007/s00253-012-4208-8.

64. Palmer JM, Keller NP. 2010. Secondary metabolism in fungi: does chromosomal location matter? Curr Opin Microbiol 13:431–436. https://doi.org/10.1016/j.mib.2010.04.008.

65. Soukup AA, Chiang YM, Bok JW, Reyes-Dominguez Y, Oakley BR, Wang CCC, Strauss J, Keller NP. 2012. Overexpression of the *Aspergillus nidulans* histone 4 acetyltransferase EsaA increases activation of secondary metabolite production. Mol Microbiol 86:314–330. https://doi.org/10.1111/j.1365-2958.2012.08195.x.

66. Albright JC, Henke MT, Soukup AA, McClure RA, Thomson RJ, Keller NP, Kelleher NL. 2015. Large-scale metabolomics reveals a complex response of *Aspergillus nidulans* to epigenetic perturbation. ACS Chem Biol 10:1535–1541. https://doi.org/10.1021/acschembio.5b00025.

67. Shwab EK, Bok JW, Tribus M, Galehr J, Graessle S, Keller NP. 2007. Histone deacetylase activity regulates chemical diversity in *Aspergillus*. Eukaryot Cell 6:1656–1664. https://doi.org/10.1128/EC.00186-07.

68. Shimizu K, Keller NP. 2001. Genetic involvement of a cAMP-dependent protein kinase in a G protein signaling pathway regulating morphological and chemical transitions in *Aspergillus nidulans*. Genetics 157:591–600.

69. Yu JH, Hamari Z, Han KH, Seo JA, Reyes-Domínguez Y, Scazzocchio C. 2004. Double-joint PCR: a PCR-based molecular tool for gene manipulations in filamentous fungi. Fungal Genet Biol 41:973–981. https://doi.org/10.1016/j.fgb.2004.08.001.

70. Sieńko M, Paszewski A. 1999. The *metG* gene of *Aspergillus nidulans* encoding cystathionine beta-lyase: cloning and analysis. Curr Genet 35:638–646. https://doi.org/10.1007/s002940050463.

71. van Leeuwen J, Andrews B, Boone C, Tan G. 2015. Rapid and efficient plasmid construction by homologous recombination in yeast. Cold Spring Harb Protoc 2015:pdb.prot085100. https://doi.org/10.1101/pdb.prot085100.

72. Livak KJ, Schmittgen TD. 2001. Analysis of relative gene expression data using real-time quantitative PCR and the 2(-Delta Delta C(T)) method. Methods 25:402–408. https://doi.org/10.1006/meth.2001.1262.

73. Maggio-Hall LA, Wilson RA, Keller NP. 2005. Fundamental contribution of β-oxidation to polyketide mycotoxin production *in planta*. Mol Plant Microbe Interact 18:783–793. https://doi.org/10.1094/MPMI-18-0783.

74. Qiao F, Bowie JU. 2005. The many faces of SAM. Sci STKE 2005:re7. https://doi.org/10.1126/stke.2862005re7.

75. Cozier GE, Carlton J, Bouyoucef D, Cullen PJ. 2004. Membrane targeting by pleckstrin homology domains. Curr Top Microbiol Immunol 282:49–88. https://doi.org/10.1007/978-3-642-18805-3_3.